Evidence for adaptive evolution in the receptor-binding domain of seasonal coronaviruses OC43 and 229E

Kathryn E. Kistler*[1,2], Trevor Bedford[1,2]

[1]*Vaccine and Infectious Disease Division, Fred Hutchinson Cancer Research Center, Seattle, WA USA*
[2]*Molecular and Cellular Biology Program, University of Washington, Seattle, WA USA*
* To whom correspondence should be addressed.

Abstract
Seasonal coronaviruses (OC43, 229E, NL63 and HKU1) are endemic to the human population, regularly infecting and reinfecting humans while typically causing asymptomatic to mild respiratory infections. It is not known to what extent reinfection by these viruses is due to waning immune memory or antigenic drift of the viruses. Here, we address the influence of antigenic drift on immune evasion of seasonal coronaviruses. We provide evidence that at least two of these viruses, OC43 and 229E, are undergoing adaptive evolution in regions of the viral spike protein that are exposed to human humoral immunity. This suggests that reinfection may be due, in part, to positively-selected genetic changes in these viruses that enable them to escape recognition by the immune system. It is possible that, as with seasonal influenza, these adaptive changes in antigenic regions of the virus would necessitate continual reformulation of a vaccine made against them.

Introduction
Coronaviruses were first identified in the 1960s and, in the decades that followed, human coronaviruses (HCoVs) received a considerable amount of attention in the field of infectious disease research. At this time, two species of HCoV, OC43 and 229E, were identified as the causative agents of roughly 15% of common colds (McIntosh 1974; Heikkinen and Järvinen 2003). Infections with these viruses were shown to exhibit seasonal patterns, peaking in January-March in the Northern Hemisphere, as well as yearly variation, with the greatest incidence occurring every 2-4 years (Monto and Lim 1974; Hamre and Beem 1972). Subsequently, two additional seasonal HCoVs, HKU1 and NL63, have entered the human population. These 4 HCoVs endemic to the human population usually cause mild respiratory infections, but occasionally result in more severe disease in immunocompromised patients or the elderly (D. X. Liu, Liang, and Fung 2020). In the past 20 years, three additional HCoVs (SARS-CoV-1, MERS-CoV and SARS-CoV-2) have emerged, which cause more severe respiratory illness. At the writing of this paper, amidst the SARS-CoV-2 pandemic, no vaccine for any HCoV is currently available, though many candidate SARS-CoV-2 vaccines are in production and clinical trials (Krammer 2020).

Coronaviruses are named for the ray-like projections of spike protein that decorate their surface. Inside these virions is a positive-sense RNA genome of roughly 30kB (F. Li 2016). This large genome size can accommodate more genetic variation than a smaller genome (Woo et al.

2009). Genome flexibility, coupled with a RNA virus error-prone polymerase (Drake 1993) and a high rate of homologous recombination (Pasternak, Spaan, and Snijder 2006), creates genetic diversity that is acted upon by evolutionary pressures that select for viral replication. This spawns much of the diversity within and between coronaviruses species (Woo et al. 2009; Hon et al. 2008), and can contribute to the virus' ability to jump species-barriers, allowing a previously zoonotic CoV to infect and replicate in humans.

The battle between virus and host results in selective pressure for mutations that alter viral antigens in a way that evades immune recognition. Antigenic evolution, or antigenic drift, leaves a characteristic mark of positively selected epitopes within the viral proteins most exposed to the host immune system (Smith et al. 2004). For CoVs, this is the spike protein, exposed on the surface of the virion to human humoral immunity. Some human respiratory illnesses caused by RNA viruses, like seasonal influenza (Smith et al. 2004), evolve antigenically, while others, like measles, do not (Fulton et al. 2015a). Because of this, seasonal influenza vaccines must be reformulated on a nearly annual basis, while measles vaccines typically provide lifelong protection. Whether HCoVs undergo antigenic drift is relevant not only to understanding HCoV evolution and natural immunity against HCoVs, but also to predicting the duration of a vaccine's effectiveness.

Early evidence that closely-related HCoVs are antigenically diverse comes from a 1980s human challenge study in which subjects were infected and then reinfected with a variety of 229E-related strains (Reed 1984). All subjects developed symptoms and shed virus upon initial virus inoculation. After about a year, subjects who were re-inoculated with the same strain did not show symptoms or shed virus. However, the majority of subjects who were re-inoculated with a heterologous strain developed symptoms and shed virus. This suggests that immunity mounted against 229E viruses provides protection against some, but not all, other 229E strains. This is a result that would be expected of an antigenically evolving virus.

More recent studies have identified 8 OC43 genotypes and, in East Asian populations, certain genotypes were shown to temporally replace other genotypes (Lau et al. 2011; Y. Zhang et al. 2015; Zhu et al. 2018). Whether certain genotypes predominate due to antigenic differences that confer a fitness advantage is not known. However, evidence for selection in the spike protein of one of these dominant OC43 genotypes has been provided by *dN/dS*, a standard computational method for detecting positive selection (Ren et al. 2015). This method has also been used to suggest positive selection in the spike protein of 229E (Chibo and Birch 2006). Additionally, two genetically distinct groupings (each of which include multiple of the aforementioned 8 genotypes) of OC43 viruses have been shown to alternate in prevalence within a Japanese community, meaning that the majority of OC43 infections are caused by one group for about 2-4 years at which point the other group begins to account for the bulk of infections. It has been suggested that antigenic differences between these groups contribute to this epidemic switching (Komabayashi et al. 2020).

However, a similar surveillance of the NL63 genotypes circulating in Kilifi, Kenya found that NL63 genotypes persist for relatively long periods of time, that people become reinfected by the

same genotype, and that reinfections are often enhanced by prior infection (Kiyuka et al. 2018). These findings are inconsistent with antigenic evolution in NL63.

Here, we use a variety of computational approaches to detect adaptive evolution in spike and comparator proteins in HCoVs. These methods were designed as improvements to *dN/dS* with the intention of identifying adaptive substitutions within a serially-sampled RNA virus population. We focus on the seasonal HCoVs that have been continually circulating in humans: OC43, 229E, HKU1 and NL63. Our analyses of nonsynonymous divergence, rate of adaptive substitutions, and Time to Most Recent Ancestor (TMRCA) provide evidence that the spike protein of OC43 and 229E is under positive selection. Though we conduct these analyses on HKU1 and NL63, we do not observe evidence for adaptive evolution in the spike protein of these viruses. For HKU1, there is not enough longitudinal sequencing data available for us to confidently make conclusions as to whether or not this lack of evidence reflects an actual lack of adaptive evolution.

Results

Phylogenetic consideration of viral diversity and recombination in OC43 and 229E

We constructed time-resolved phylogenies of the OC43 and 229E using publicly accessible sequenced isolates. A cursory look at these trees confirms previous reports that substantial diversity exists within each viral species (Y. Zhang et al. 2015; Komabayashi et al. 2020; Lau et al. 2011). Additionally, the trees form ladder-like topologies with isolate tips arranged into temporal clusters rather than geographic clusters, indicating a single global population rather than geographically-isolated populations of virus. The phylogeny of OC43 bifurcates immediately from the root (Figure 1), indicating that OC43 consists of multiple, co-evolving lineages. Because of the distinct evolutionary histories, it is appropriate to conduct phylogenetic analyses separately for each lineage. We have arbitrarily labeled these lineages ‘A’ and ‘B’ (Figure 1).

Because recombination is common amongst coronaviruses (Pasternak, Spaan, and Snijder 2006; Hon et al. 2008; Lau et al. 2011), we built separate phylogenies for each viral gene. In the absence of recombination, each tree should show the same evolutionary relationships between viral isolates. A dramatic difference in a given isolate’s position on one tree versus another is strongly indicative of recombination (Kosakovsky Pond et al. 2006). Comparing the RNA-dependent RNA polymerase (RdRp) and spike trees reveals this pattern of recombination in some isolates (Figure 1- figure supplement 1A). A comparison of the trees of the S1 and S2 sub-domains of spike shows more limited evidence for intragenic recombination (Figure 1-figure supplement 1B), which is consistent with the fact that the distance between two genetic loci is inversely-related to the chance that these loci remain linked during a recombination event. Though intragenic recombination likely does occur occasionally, analyzing genes, rather than isolates, greatly reduces the contribution of recombination to genetic variation in our analyses.

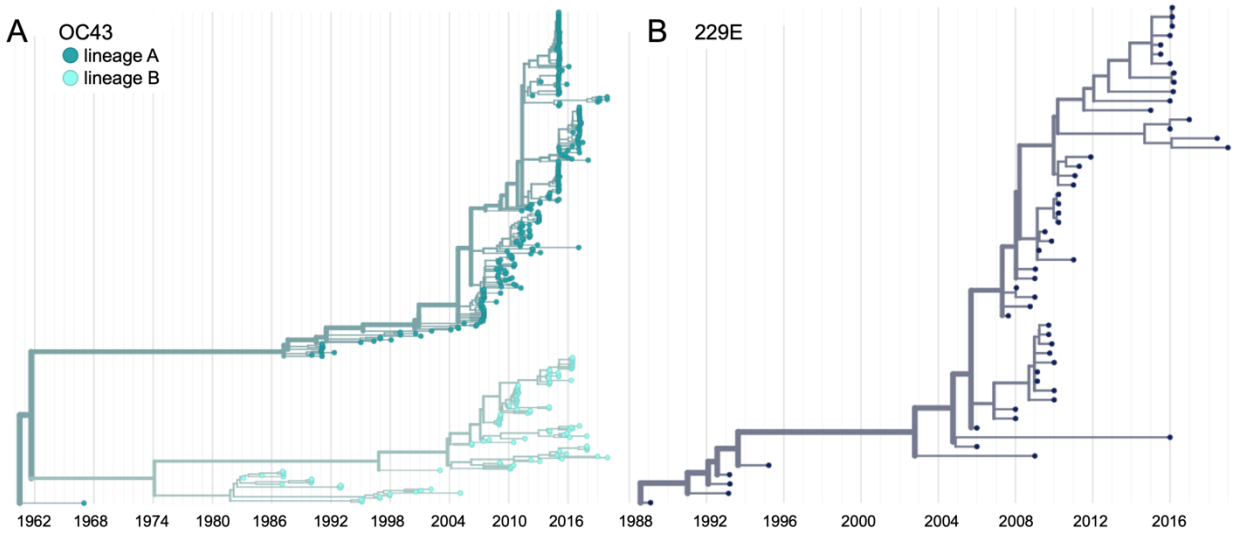

Figure 1. Phylogenetic trees for spike gene of seasonal HCoVs OC43 and 229E. Phylogenies built from A: OC43 spike sequences from 389 isolates over 53 years, and B: 229E spike sequences from 54 isolates over 31 years. OC43 bifurcates immediately after the root and is split into two lineages: lineage A (dark teal) and lineage B (light teal). 229E and contains just one lineage (dark blue). For the analyses in this paper, the evolution of each gene (or genomic region) is considered separately, so phylogenies are built for each viral gene, and those phylogenies are used to split isolates into lineages for each gene. These are temporally resolved phylogenies with year shown on the x-axis. The clock rate estimate is 5×10^{-4} substitutions per nucleotide site per year for OC43 and 6×10^{-4} for 229E.

Thus, in all of our analyses, we use alignments and phylogenies of sequences of single genes (or genomic regions) rather than whole genome sequences of isolates. We designate the lineage of those genes (or genomic regions) based on the gene's phylogeny. Though most isolates contain all genes from the same lineage, some isolates have, say, a lineage A spike gene and a lineage B RdRp gene. This strategy allows us to consider the evolution of each gene separately, and interrogate the selective pressures acting on them.

It is worth noting that the analyses we use here to detect adaptive evolution canonically presume that selective pressures are acting on single nucleotide polymorphisms (SNPs). However, it is possible that recombination also contributes to the genetic variation that is acted on by immune selection. This would be most likely to occur if two closely-related genomes recombine, resulting in the introduction of a small amount of genetic diversity without disrupting crucial functions. Our analyses do not aim to determine the source of genetic variation (i.e. SNPs or recombination), but rather focus on identifying if and how selection acts on this variation.

Because of its essential role in viral replication and lack of antibody exposure, we expect RdRp to be under purifying selection to maintain its structure and function. If HCoVs evolve antigenically, we expect to see adaptive evolution in spike, and particularly in the S1 domain of spike (Hofmann et al. 2006; Hulswit et al. 2019), due to its exposed location at the virion's surface and interaction with the host receptor. Mutations that escape from population immunity are beneficial to the virus and so are driven to fixation by positive selection. This results in adaptive evolution of the virus population.

Phylogenetic inference of substitution prevalence within spike

Using phylogenies constructed from the spike gene, we tallied the number of independent amino acid substitutions at each position within spike. The average number of substitutions per site is higher in S1 than S2 for HCoV lineages in OC43 and 229E (Figure 2A). We focus on S1 rather than the Receptor-Binding Domain (RBD) within S1 in our analyses, because it is known that neutralizing antibodies bind to epitopes within the N-Terminal Domain (NTD) as well as the RBD of S1 (L. Liu et al. 2020; S. Zhang et al. 2018; Zhou et al. 2019). A greater occurrence of repeated substitutions is expected if some mutations within S1 confer immune avoidance. Alternatively, these repeated substitutions could be a result of high mutation rate and random genetic drift as has been shown at particular types of sites in SARS-CoV-2 (van Dorp et al. 2020). However, this latter hypothesis should affect all regions of the genome equally and should not result in a greater number of repeated substitutions in S1 than S2.

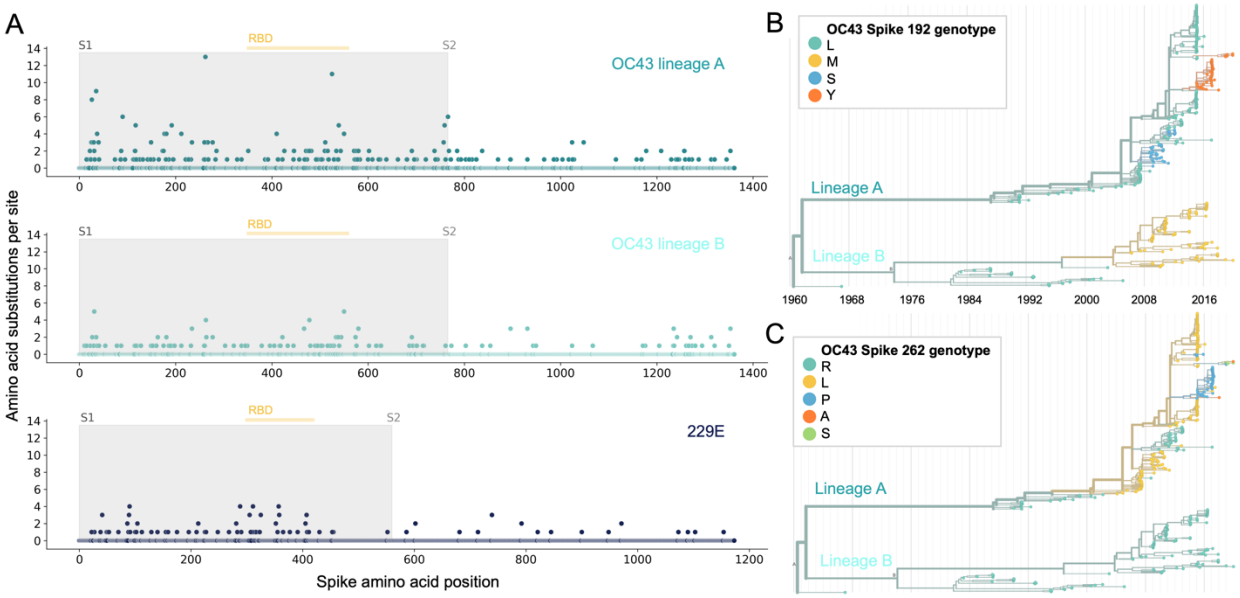

Figure 2. More sites mutate repeatedly within spike S1 versus S2. A: Number of substitutions observed at each amino acid position in the spike gene throughout the phylogeny. S1 (gray) and S2 (white) are indicated by shading and the number of substitutions per site is indicated by a dot and color-coded by HCoV lineage. The putative receptor-binding domains for 229E (Z. Li et al. 2019) and the putative domain for OC43 (Lau et al. 2011) are indicated with light yellow bars. Asterisks indicate two example positions (192 and 262), which mutate repeatedly throughout the OC43 lineage A phylogeny. The OC43 phylogeny built from spike sequences and color-coded by genotype at position 192 and 262 is shown in B) and C), respectively.

If the repeated mutations are a product of immune selection, not only should S1 contain more repeated mutations, but we would also expect these mutations to spread widely after they occur due to their selective advantage. Additionally, we expect sites within S1 to experience diversifying selection due to the ongoing arms race between virus and host immune system. This is visible in the distribution of genotypes at the most repeatedly-mutated sites in OC43 lineage A (Figure 2B and 2C).

Nonsynonymous and synonymous divergence in RdRp and subdomains of spike

An adaptively evolving gene, or region of the genome, should exhibit a high rate of nonsynonymous substitutions. For each seasonal HCoV lineage, we calculated nonsynonymous and synonymous divergence as the average Hamming distance from that lineage's most recent common ancestor (Zanini et al. 2015). The rate of nonsynonymous divergence is markedly higher within spike versus RdRp of 229E and OC43 lineage A (Figure 3A). While nonsynonymous divergence increases steadily over time in spike, it remains roughly constant at 0.0 in RdRp. These results suggest that there is predominantly positive selection on OC43 and 229E spike, but predominantly purifying selection on RdRp. Separating spike into the S1 (receptor-binding) and S2 (membrane-fusion) domains reveals that the majority of nonsynonymous divergence in spike occurs within S1 (Figure 3B). In fact, the rates of nonsynonymous divergence in S2 are similar to those seen in RdRp, suggesting S2 evolves under purifying selection while S1 evolves adaptively.

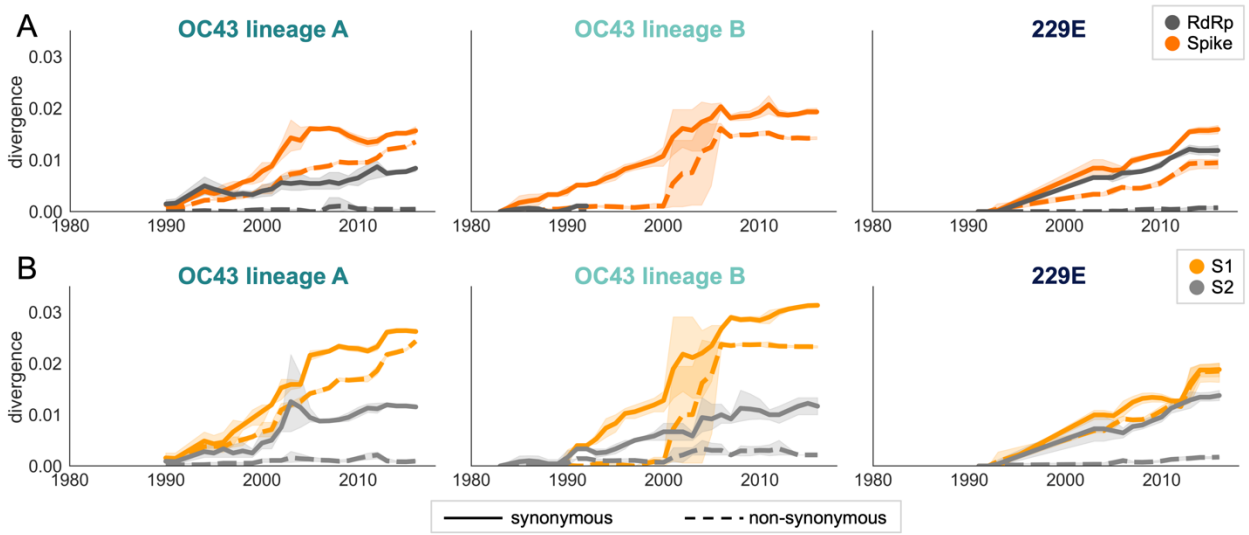

Figure 3. Nonsynonymous divergence is higher in OC43 and 229E Spike S1 versus S2 or RdRp. A: Nonsynonymous (dashed lines) and synonymous divergence (solid lines) of the spike (dark orange) and RdRp (dark gray) genes of all 229E and OC43 lineages over time. Divergence is the average Hamming distance from the ancestral sequence, computed in sliding 3-year windows which contain at least 2 sequenced isolates. Shaded region shows 95% confidence intervals. Note that the absence of a line means there fewer than 2 sequences available at this timepoint and that, therefore, the divergence is not calculated. B: Nonsynonymous and synonymous divergence within the S1 (light orange) and S2 (light gray) domains of spike. Year is shown on the x-axis and is shared between plots.

Though we would expect synonymous divergence to be equivalent in all areas of the genome, this is not born out in our results. It is unclear whether the difference in synonymous divergence between genes reflects an actual biological difference. However, the ratio of nonsynonymous divergence in spike to nonsynonymous divergence in RdRp is consistently higher than the equivalent ratio of synonymous divergence (Figure 3- figure supplement 2). Thus, despite differences in synonymous divergence, spike is accumulating more relatively more nonsynonymous divergence than RdRp.

We compared our analysis of divergence to the results a more standard approach for detecting positive selection on certain branches of a phylogeny. This approach, called MEME, is maximum-likelihood method which gives a single *dN/dS* value for each gene (Murrell et al. 2012; Weaver et al. 2018). In agreement with measures of nonsynonymous divergence over time, *dN/dS* estimates are higher in Spike than RdRp and higher in S1 than S2 (Table 2). Our estimate of *dN/dS* in OC43 spike is similar to the previously reported estimate of roughly 0.3 (Ren et al. 2015). However, we believe the standard *dN/dS* approach is not the ideal tool for detecting adaptive evolution in HCoVs because it is a phylogenetic approach, which may be biased by recombination, and also because some assumptions of the model hold true for mammalian genomes, but not necessarily for RNA viruses.

	RdRp	**Spike**	**S1**	**S2**
229E	0.143	0.441	0.662	0.166
OC43 lineage A	0.080	0.435	0.466	0.301
OC43 lineage B	0.061	0.317	0.418	0.234
NL63	0.068	0.139	0.121	0.038

Table 1. dN/dS is lower in Spike than RdRp. A single *dN/dS* value was computed for gene (or spike domain) and each HCoV using MEME.

Rate of Adaptation in RdRp and subdomains of spike

Therefore, as a complement to the divergence analysis, we implemented an alternative to the *dN/dS* method that was specifically designed to detect positive selection within RNA virus populations (Bhatt, Holmes, and Pybus 2011). Compared with traditional *dN/dS* methods, the Bhatt method has the advantages of: 1) measuring the strength of positive selection within a population given sequences collected over time, 2) higher sensitivity to identifying mutations that occur only once and sweep through the population, and 3) correcting for deleterious mutations (Bhatt, Katzourakis, and Pybus 2010; Bhatt, Holmes, and Pybus 2011). Briefly, this method defines a class of neutrally-evolving nucleotide sites as those with synonymous mutations or where nonsynonymous polymorphisms occur at medium frequency. Then, the number of fixed and high-frequency nonsynonymous sites that exceed the neutral expectation are calculated. This method compares nucleotide sequences at each timepoint (the ingroup) to the consensus nucleotide sequence at the first time point (the outgroup) and yields an estimate of the number of adaptive substitutions within a given genomic region at each of these timepoints.

We adapted this method to detect adaptive substitutions in seasonal HCoVs. As shown in Figure 4, OC43 lineage A has continuously amassed adaptive substitutions in spike over the past >30 years while RdRp has accrued few, if any, adaptive substitutions. These adaptive substitutions are located within the S1, and not the S2, domain of spike (Figure 4). We observe a largely linear accumulation of adaptive substitutions in spike and S1 through time, although the method does not dictate a linear increase. This observation suggests that spike (and S1 in particular) is evolving in response to a continuous selective pressure. This is exactly what would

be expected if these adaptive substitutions are evidence of antigenic evolution resulting from an evolutionary arms race between spike and the host immune system.

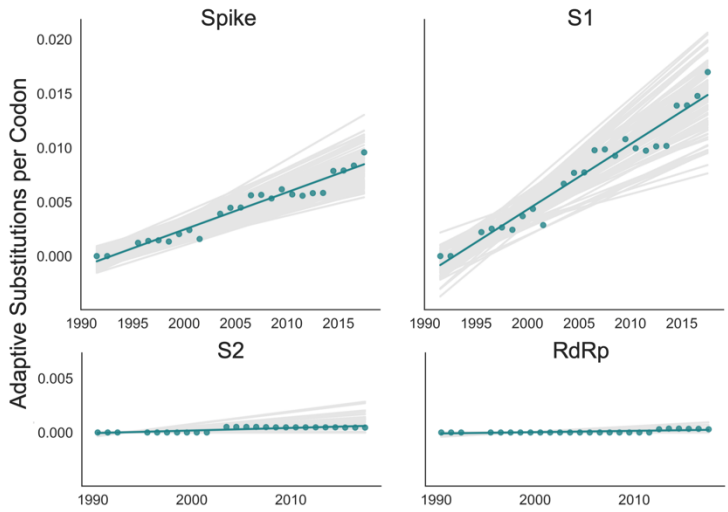

Figure 4. Adaptive substitutions accumulate over time in OC43 lineage A spike S1. Adaptive substitutions per codon within OC43 lineage A spike, S1, S2 and RdRp as calculated by our implementation of the Bhatt method. Adaptive substitutions are computed in sliding 3-year windows, and only for timepoints that contain 3 or more sequenced isolates. Red dots display estimated values calculated from the empirical data and red lines show linear regression fit to these points. Grey lines show the distribution of regressions fit to the computed number of adaptive substitutions from 100 bootstrapped datasets. Year is shown on the x-axis.

We estimate that OC43 lineage A accumulates roughly 0.61×10^{-3} adaptive substitutions per codon per year (or 0.45 adaptive amino acid substitutions in S1 each year) in the S1 domain of spike, while the rate of adaptation in OC43 lineage B is slightly higher and is estimated to result in an average 0.56 adaptive substitutions in S1 per year (Figure 5). The S1 domain of 229E is estimated to accrue 0.26 adaptive substitutions per year (a rate of 0.47×10^{-3} adaptive substitutions per codon per year).

A benefit of the Bhatt method is the ability to calculate the strength of selection, which allows us to compare these seasonal HCoVs to other viruses. We used our implementation of the Bhatt method to calculate the rate of adaptation for influenza A/H3N2, which is known to undergo rapid antigenic evolution (Rambaut et al. 2008; Yang 2000), measles, which does not (Fulton et al. 2015a), and influenza B strains Vic and Yam, which evolve antigenically at a slower rate than A/H3N2 (Bedford et al. 2014). We estimate that the receptor-binding domain of influenza A/H3N2 accumulates adaptive substitutions between 2 and 3 times faster than the HCoVs OC43 and 229E (Figure 6). The rate of adaptive substitution in influenza B/Yam and B/Vic are on par with the seasonal HCoVs. We detect no adaptive substitutions in the measles receptor-binding protein. These results put the evolution of the S1 domain of OC43 and 229E in context, indicating that the S1 domain is under positive selection, and that this positive selection generates new variants in the putative antigenic regions of these HCoVs at about the same rate as influenza B strains and about half the rate of the canonical example of antigenic evolution, the HA1 domain of influenza A/H3N2.

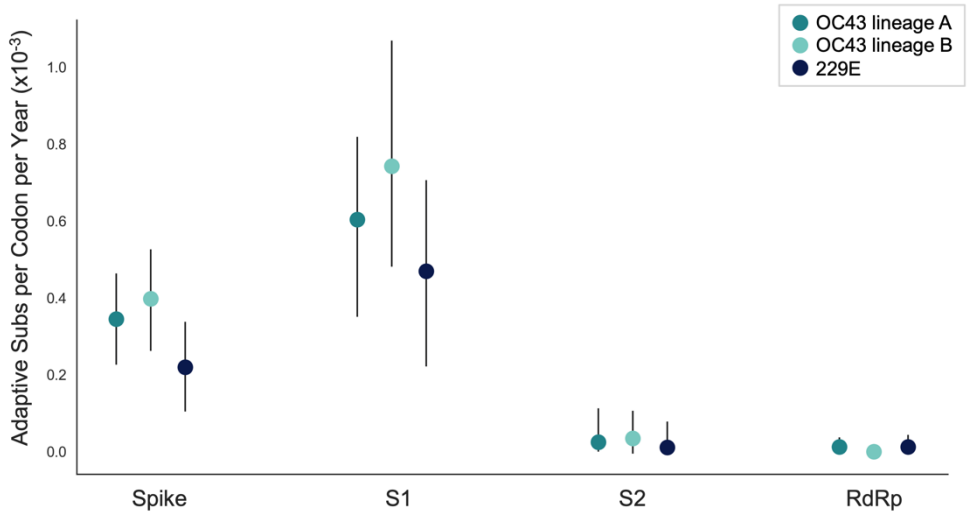

Figure 5. The rate of adaptive substitution is highest in spike S1. Adaptive substitutions per codon per year as calculated by our implementation of the Bhatt method. Rates are calculated within Spike, S1, S2 and RdRp for 229E and OC43 lineages. Error bars show 95% bootstrap percentiles from 100 bootstrapped datasets.

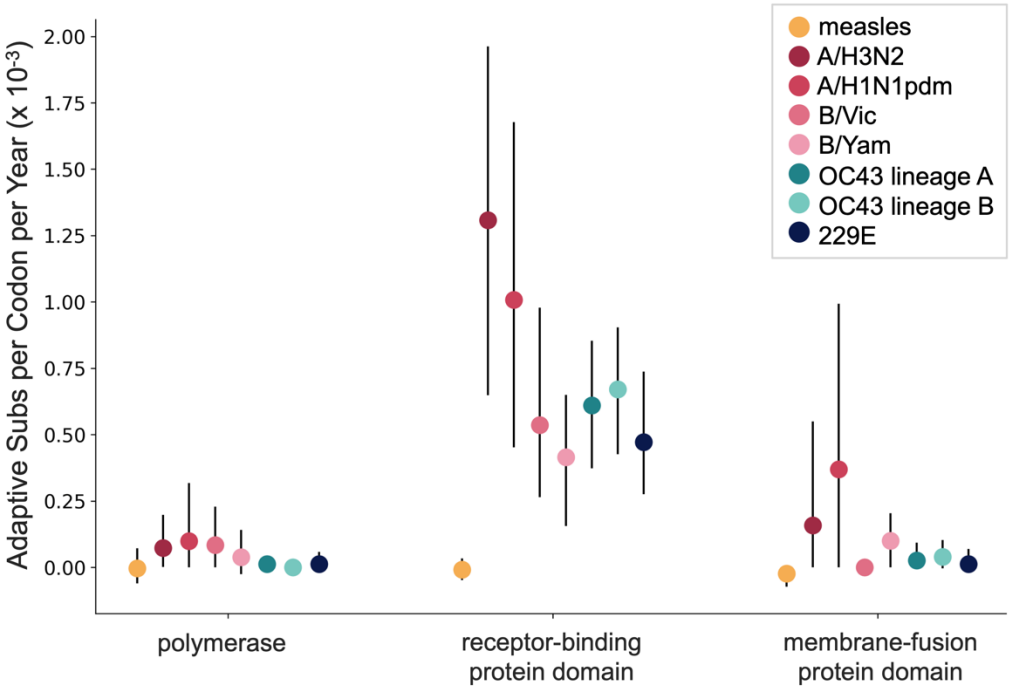

Figure 6. OC43 and 229E spike S1 accumulates adaptive substitutions faster than measles but slower than influenza A/H3N2. Comparison of adaptive substitutions per codon per year between measles (yellow), 4 influenza strains (A/H3N2, A/H1N1pdm, B/Vic and B/Yam- shown in shades of red), OC43 lineage A (dark teal), OC43 lineage B (light teal), and 229E (dark blue). The polymerase, receptor binding domain and membrane fusion domain for influenza strains are PB1, HA1 and HA2. For both HCoVs, they are RdRp, S1 and S2, respectively. For measles, the polymerase is the P gene, the receptor-binding protein is the H gene and the fusion protein is the F gene. Error bars show 95% bootstrap percentiles from 100 bootstrapped datasets.

Validation that rate of adaptation is not biased by recombination

Because coronaviruses are known to recombine, and recombination has the potential to impact evolutionary analyses of selection, we sought to verify that our results are not swayed by the presence of recombination. To do this, we simulated the evolution of OC43 lineage A spike and RdRp genes under varying levels of recombination and positive selection (representative phylogenies of simulated spike evolution can be seen in Figure 7- figure supplement 2) and used our implementation of the Bhatt method to identify adaptive evolution. As the strength of positive selection increases, we detect a higher rate of adaptive evolution, regardless of the level of recombination (Figure 7). This demonstrates that our estimates of adaptive evolution are not biased by recombination events.

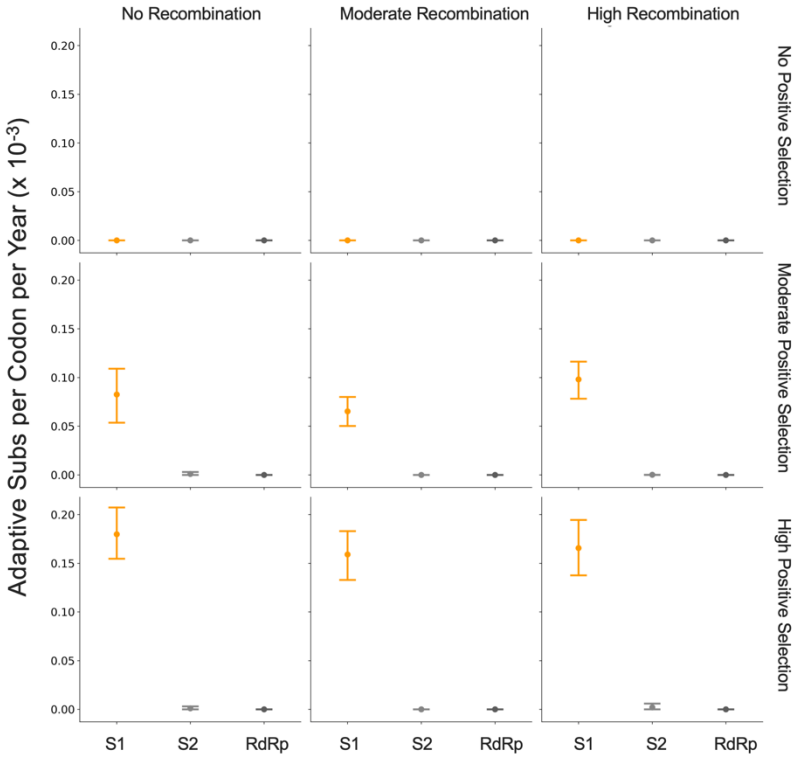

Figure 7. Detection of positive selection is not biased by recombination. OC43 lineage A sequences were simulated with varying levels of recombination and positive selection. The Bhatt method was used to calculate the rate of adaptive substitutions per codon per year for S1 (light orange), S2 (light gray) and RdRp (dark gray). The mean and 95% confidence interval of 10 independent simulations is plotted.

Time to Most Recent Common Ancestor (TMRCA) of RdRp and subdomains of spike

Finally, we know that strong directional selection skews the shape of phylogenies (Volz, Koelle, and Bedford 2013). In influenza H3N2, immune selection causes the genealogy to adopt a ladder-like shape where the rungs are formed by viral diversification and each step is created by the appearance of new, antigenically-superior variants that replace previous variants. This ladder-like shape can also be seen in the phylogenies of the OC43 and 229E (Figure 1). In this case, selection can be quantified by the timescale of population turnover as measured by the Time to Most Recent Common Ancestor (TMRCA), with the expectation that stronger selection

will result in more frequent steps and therefore a smaller TMRCA measure (Bedford, Cobey, and Pascual 2011). We computed average TMRCA values from phylogenies built on Spike, S1, S2 or RdRp sequences of OC43 lineage A and 229E (Table 2). We did not compute TMRCA for OC43 lineage B because the limited number of available RdRp sequences for this lineage mean that TMRCA can only be calculated for about 4 years, which could artificially skew the TMRCA estimates. Our estimates of HCoV spike TMRCA are roughly 2-2.5 longer the estimated TMRCA for influenza A/H3N2 hemagglutinin (Bedford, Cobey, and Pascual 2011).

We observe that, for both OC43 lineage A and 229E, the average TMRCA is lower in spike than RdRp and lower in S1 versus S2. These results suggest strong directional selection in S1, likely driven by pressures to evade the humoral immune system. The difference in TMRCA between S1 and S2 is indicative not only of differing selective pressures acting on these two spike domains, but also of intra-spike recombination. This is because the immune selection imposed on S1, should also propagate neutral hitch-hiker mutations in closely-linked regions such as S2. The difference in TMRCA suggests that recombination may uncouple these regions. Recombination can also push TMRCA to higher values, though this should not have a larger impact on RdRp than S1. The contributions of the forces of directional selection and recombination are difficult to parse from the TMRCA results. This emphasizes the importance of using methods, such as the Bhatt method, that are robust to recombination to detect adaptive evolution.

	Spike	**S1**	**S2**	**RdRp**
OC43 lineage A	4.67 (4.04, 5.28)	3.45 (2.86, 4.05)	13.05 (11.24, 14.97)	17.39 (15.63, 19.15)
229E	4.19 (3.13, 5.25)	2.23 (1.76, 2.69)	5.08 (3.93, 6.23)	4.86 (4.04, 5.69)

Table 2. Mean TMRCA is lower in S1 than RdRp or S2. Average TMRCA values (in years) for OC43 lineage A and 229E. The 95% confidence intervals are indicated in parentheses below mean TMRCA values.

Application of methods for identifying adaptive evolution to HKU1 and NL63

Because HKU1 was identified in the early 2000's, there are fewer longitudinally-sequenced isolates available for this HCoV compared to 229E and OC43 (Figure 1- figure supplement 2). Consequently, the phylogenetic reconstructions and divergence analysis of HKU1 have a higher level of uncertainty. To begin with, it is less clear from the phylogenies whether HKU1 represents a single HCoV lineage like 229E or, instead, should be split into multiple lineages like OC43 (Figure 1). Because of this, we completed all antigenic analyses for HKU1 twice: once considering all isolates to be members of a single lineage, and again after splitting isolates into 2 separate lineages. These lineages are arbitrarily labeled 'A' and 'B' as was done for OC43. When HKU1 is considered to consist of just one lineage, there is no signal of antigenic evolution by divergence analysis (Figure 3- figure supplement 1B) or by the Bhatt method of estimating adaptive evolution (Figure 5- figure supplement 1A). However, when HKU1 is assumed to consist of 2 co-circulating lineages, HKU1 lineage A has a markedly higher rate of adaptive substitutions in S1 than in S2 or RdRp (Figure 5- figure supplement 1B).

To demonstrate the importance of having a well-sampled longitudinal series of sequenced isolates for our antigenic analyses, we returned to our simulated OC43 S1 datasets. We mimicked shorter longitudinal series by truncating the dataset to only 24, 14, 10, or 7 years of samples and ran the Bhatt analysis on these sequentially shorter time series (Figure 7- figure supplement 1). The rates of adaptation estimated from the truncated datasets can be compared to the "true" rate of adaptation calculated from all simulated data. This simulated data reveals a general trend that less longitudinal data reduces the ability to detect adaptive evolution by skewing the estimated rate away from the "truth" and increasing the uncertainty of the analysis. Given the dearth of longitudinal data for HKU1, we do not feel that it is appropriate to make strong conclusions about adaptive evolution, or lack thereof, in this HCoV.

Despite being identified at roughly the same time as HKU1, substantially more NL63 isolates have been sequenced (Figure 1- figure supplement 2) making the phylogenetic reconstruction and evolutionary analyses of this virus correspondingly more reliable. We do not observe evidence for adaptive evolution in NL63 (Figure 3- figure supplement 1A and Figure 5- figure supplement 1A) and this lack of support for adaptive evolution in the NL63 spike gene is more likely to reflect an actual lack of adaptive evolution in this virus.

Discussion

Using several corroborating methods, we provide evidence that the seasonal HCoVs OC43 and 229E undergo adaptive evolution in S1, the region of the spike protein exposed to human humoral immunity (Figures 3, 4 and 5). We additionally confirm that RdRp and S2 do not show signals of adaptive evolution. We observe that S1 accumulates between 0.3 (229E) and 0.5 (OC43) adaptive substitutions per year. We infer that these viruses accumulate adaptive substitutions at roughly half the rate of influenza A/H3N2 and at a similar rate to influenza B viruses (Figure 6). The most parsimonious explanation for the observation of substantial adaptive evolution in S1 is that antigenic drift is occurring in which mutations that escape from human population immunity are selectively favored in the viral population leading to repeated adaptive changes. However, it is formally possible that the adaptive evolution we detect is a result of selective pressures other than evasion of the adaptive immune system. Showing that this is truly antigenic evolution could involve a serological comparison of isolates that differ at S1 residues under positive selection.

In seasonal influenza and measles, the rates of adaptive evolution we estimate correlate well with relative rates of antigenic drift reported by other groups (Fulton et al. 2015b; Bedford et al. 2014). The relative rates of adaptation we calculate also match the relative frequency of vaccine strain updates, as would be expected since vaccines must be updated to match antigenically-evolving viruses. Since 2006, the A/H3N2 component of the seasonal influenza vaccine has been updated 10 times (11 different A/H3N2 strains), 4 different B/Vic strains and 4 different B/Yam strains have been included in the vaccine, and the measles vaccine strain has not changed (Global Influenza Surveillance and Response System (GISRS), https://www.who.int/influenza/vaccines/virus/en/). Using these numbers as guidance,

our results suggest that a vaccine against OC43 or 229E might need to be updated as frequently as the B/Vic and B/Yam components of the influenza vaccine are.

We do not observe evidence of antigenic evolution in NL63 (Figure 3-figure supplement 1 and Figure 5- figure supplement 1). This likely represents a lack of marked adaptive evolution in S1. Our finding fits with a study of NL63 in Kenya, which identified multiple genotypes of NL63 and show that people regularly become reinfected with the same genotype of NL63 (Kiyuka et al. 2018). Additionally, Kiyuka et al found that these genotypes circulate locally for a long period of time, suggesting a decent amount of viral diversity and a potential lack of evolution due to immune selection. Though our results cannot explain why OC43 and 229E likely evolve antigenically while NL63 does not, Kiyuka et al observe that NL63 reinfections are sometimes enhanced by a previous infection and hypothesize that NL63 is actually under purifying selection at epitope sites (Kiyuka et al. 2018).

Though analysis of all HCoVs would benefit from more sequenced isolates, there is substantially less longitudinal sequencing data available for HKU1. Thus, despite finding no evidence of antigenic evolution in HKU1 (Figure 3-figure supplement 1 and Figure 5- figure supplement 1), it is possible that a more completely sampled time series of HKU1 genome sequences could alter the result for this virus (Figure 7-figure supplement 1).

Our conclusions of adaptive evolution in S1, arrived at through computational analyses of sequencing data, agree with studies that observe reinfection of subjects by heterologous isolates of 229E (Reed 1984), sequential dominance of specific genotypes of OC43 (Lau et al. 2011; Y. Zhang et al. 2015), and common reinfection by seasonal HCoVs from longitudinal serological data (Edridge et al. 2020). In this latter study, HCoV infections were identified from longitudinal serum samples by assaying for increases in antibodies against the nucleocapsid (N) protein of representative OC43, 229E, HKU1, and NL63 viruses. This study concluded that the average time between infections was 1.5–2.5 years, depending on the HCoV (Edridge et al. 2020). In comparison, influenza H3N2 reinfects people roughly every 5 years (Kucharski et al. 2015). Thus, frequent reinfection by seasonal HCoVs is likely due to a combination of factors and suggests waning immune memory, and/or incomplete immunity against reinfection, in addition to antigenic drift.

Human coronaviruses are a diverse grouping split, phylogenetically, into two genera: NL63 and 229E are alphacoronaviruses, while OC43, HKU1, MERS, SARS, and SARS-CoV-2 are betacoronaviruses. The method of cell-entry does not seem to correlate with genus. Coronaviruses bind to a remarkable range of host-cell receptors including peptidases, cell adhesion molecules and sugars. Amongst the seasonal HCoVs, OC43 and HKU1 both bind 9-O-acetylsialic acid (Hulswit et al. 2019), while 229E binds human aminopeptidase N (hAPN) and NL63 binds angiotensin-converting enzyme 2 (ACE2) (D. X. Liu, Liang, and Fung 2020). Despite a relatively large phylogenetic distance and divergent S1 structures, NL63 and SARS-CoV-1 and SARS-CoV-2 bind to the same host receptor using the same virus-binding motifs (VBMs) (F. Li 2016). This VBM is located in the C-terminal domain of S1 (S1-CTD), which fits within the trend of S1-CTD receptor-binding in CoVs that bind protein receptors (Hofmann et al.

2006; F. Li 2016). This is opposed to the trend amongst CoVs that bind sugar receptors, where receptor-binding is located within the S1 N-terminal domain (S1-NTD) (F. Li 2016). This localization roughly aligns with our observations that the majority of the repeatedly-mutated sites occur toward the C-terminal end of 229E S1 and the N-terminal end of OC43 S1 (Figure 2).

Here, we have provided support that at least 2 of the 4 seasonal HCoVs evolve adaptively in the region of spike that is known to interact with the humoral immune system. These two viruses span both genera of HCoVs, though due to the complexity of HCoV receptor-binding and pathology mentioned above, it is not clear whether or not this suggests that other HCoVs, such as SARS-CoV-2, will also evolve adaptively in S1. This is important because, at the time of writing of this manuscript, many SARS-CoV-2 vaccines are in production and most of these exclusively include spike (Krammer 2020). If SARS-CoV-2 evolves adaptively in S1 as the closely-related HCoV OC43 does, it is possible that the SARS-CoV-2 vaccine would need to be frequently reformulated to match the circulating strains, as is done for seasonal influenza vaccines.

Materials and methods

All data, source code and analyses can be found at https://github.com/blab/seasonal-cov-adaptive-evolution. All phylogenetic trees constructed and analyzed in this manuscript can be viewed interactively at https://nextstrain.org/community/blab/seasonal-cov-adaptive-evolution. All analysis code is written in Python 3 (Python Programming Language, SCR_008394) in Jupyter notebooks (Jupyter-console, RRID:SRC_018414).

Sequence data

All viral sequences are publicly accessible and were downloaded from ViPR (www.viprbrc.org) under the “Coronavirdiae” with host “human” (Pickett et al. 2012). Sequences labeled as “OC43”, “229E”, “HKU1” and “NL63” were pulled out of the downloaded FASTA file into 4 separate data files. Additionally, a phylogeny of all downloaded human coronaviruses was made and unlabeled isolates that clustered within clades formed by labeled OC43, 229E, HKU1 or NL63 isolates were marked as belonging to that HCoV type and added to our data files. Code for these data-parsing steps is located in `data-wrangling/postdownload_formatting_for_rerun.ipynb`.

Phylogenetic inference

For each of the 4 HCoV datasets, full-length sequences were aligned to a reference genome using the augur align command (Hadfield et al. 2018) and MAFFT (Katoh et al. 2002). Individual gene sequences were then extracted from these alignments if sequencing covered 50% or more of the gene using the code in `data-wrangling/postdownload_formatting_for_rerun.ipynb`. Sequence files for each gene are located in the `data/` directory within each HCoV parent directory (ex: `oc43/data/oc43_spike.fasta`). A Snakemake file (Köster and Rahmann 2012) within each HCoV directory follows the general outline of a Nextstrain build (Nextstrain, RRID:SCR_018223) and was used to align each gene to a reference strain and build a time-resolved phylogeny with IQ-Tree v1 (Nguyen et al. 2015) and TimeTree (Sagulenko, Puller, and Neher 2018).

Phylogenies were viewed to identify the distribution of genotypes throughout the tree, different lineages, and signals of recombination using the nextstrain view command (Hadfield et al. 2018). The clock rate of the phylogeny based on spike sequences for each isolate (as shown in Fig. 1 and Fig. 1 Supplement 2) was 0.0005 substitutions per nucleotide site per year for OC43, 0.0006 for 229E, 0.0007 for NL63, and 0.0062 for HKU1. All NL63 and HKU1 trees were rooted on an outgroup sequence. For NL63, the outgroup was 229e/AF304460/229e_ref/Germany/2000 and for HKU1 the outgroup was mhv/NC_048217_1/mhv/2006. Clock rates for the phylogenies built on each individual gene can be found within the `results/` directory within each HCoV parent directory (ex: `oc43/results/branch_lengths_oc43_spike.json`).

Mutation counting

Amino acid substitutions at each position in spike were tallied from the phylogeny. In other words, the phylogenetic reconstruction of spike sequences returns nucleotides changes to the ancestral sequence along each branch. The number of times this changed amino acid identity at each position was tallied. This analysis was conducted using code in `antigenic_evolution/site_mutation_rank.ipynb`.

Divergence analysis

For each HCoV lineage and each gene, synonymous and nonsynonymous divergence was calculated at all timepoints as the average Hamming distance between each sequenced isolate and the consensus sequence at the first timepoint (founder sequence). The total number of observed differences between the isolate and founder nucleotide sequences that result in nonsynonymous (or synonymous) substitutions is divided by the number of possible nucleotide mutations that result in nonsynonymous (or synonymous) substitutions, weighted by kappa, to yield an estimate of divergence. Kappa is the ratio of rates of transitions:transversions, and was calculated by averaging values from spike and RdRp trees built by BEAST 2.6.3 (Bouckaert et al. 2019) using the HKY+gamma4 model with 2 partitions and “coalescent constant population”. All BEAST results are found in `.log` files in gene- and HCoV-specific subdirectories within `beast/`. Divergence is calculated from nucleotide alignments. Sliding 3-year windows were used and only timepoints that contained at least 2 sequences were considered. The concept for this analysis is from (Zanini et al. 2015) and code for our adaptation is in `antigenic_evolution/divergence_weighted.ipynb`. The ratios of divergence shown in Figure 3- figure supplement 2 are also calculated in this notebook.

Calculation of dN/dS

A *dN/dS* value was calculated for RdRp, spike, S1 and S2 of each HCoV using the Datamonkey (Weaver et al. 2018) implementation of MEME (Mixed Effects Model of Evolution) (Murrell et al. 2012). Aligned FASTA files (ex: `oc43/results/aligned_oc43_rdrp.fasta`) were uploaded to Datamonkey (http://datamonkey.org/meme) and dN/dS value was recorded as the calculated Global MG94xREV model non-synonymous/synonymous rate ratio.

Implementation of the Bhatt method

The rate of adaptive evolution was computed using an adaptation of the Bhatt method (Bhatt, Holmes, and Pybus 2011; Bhatt, Katzourakis, and Pybus 2010). For each lineage and each genomic region, we partitioned all available sequences into sliding 3-year windows and only used timepoints that contained at least 3 sequences in the analysis. We compared nucleotide sequences at each timepoint (the ingroup) to the consensus nucleotide sequence at the first time point (the outgroup). Eight estimators (silent fixed, replacement fixed, silent high frequency, replacement high frequency, silent mid-frequency, replacement mid-frequency, silent low frequency and replacement low-frequency) are calculated by the site-counting method (Bhatt, Katzourakis, and Pybus 2010). In the site-counting method, each estimator is the product of the fixation or polymorphism score times the silent or replacement score, summed for each site in that frequency class. Fixation and polymorphism scores depend on the number of different nucleotides observed at the site and whether the outgroup base is present in the ingroup. Selectively neutral sites are assumed to contain the classes of silent polymorphisms and replacement polymorphisms occurring at a frequency between 0.15 and 0.75. A class of nonneutral, adaptive sites is then identified as having an excess of replacement fixations or polymorphisms (Bhatt, Holmes, and Pybus 2011). For each lineage and gene, 100 bootstrap alignments and ancestral sequences were generated and run through the Bhatt method to assess the statistical uncertainty of our estimates of rates of adaptation (Bhatt, Holmes, and Pybus 2011). The rate of adaptation (per codon per year) shown in Fig. 5 is calculated by linear regression of the time series values of adaptive substitutions per codon (Fig. 4). Our code for implementing the Bhatt method is at `antigenic_evolution/bhatt_bootstrapping.ipynb`.

Estimation of rates of adaptation of measles and influenza viruses

Influenza and measles alignments were generated by running Nextstrain the respective Nextstrain builds from https://github.com/nextstrain/seasonal-flu and https://github.com/nextstrain/measles (Hadfield et al. 2018). The seasonal influenza build was run with 20 year resolution for H3N2, H1N1pdm, Vic and Yam. The rates of adaptation of different genes was calculated using our implementation of the Bhatt method described above. The receptor-binding domain used for influenza was HA1, for measles was the H protein, and for the HCoVs was S1. The membrane fusion protein used for influenza was HA2, for measles was the F protein, and for the HCoVs was S2. The polymerase for influenza was PB1, for measles was the P protein, and for the HCoVs was RbRd (nsp12). Our code for this analysis is at `antigenic_evolution/bhatt_nextstrain.ipynb`.

Simulation of evolving OC43 sequences

The evolution of OC43 lineage A Spike and RdRp genes was simulated using SANTA-SIM (Jariani et al. 2019). The OC43 lineage A root sequence was used as a starting point and the simulation was run for 500 generations and 10 simulated sequences were sampled every 50 generations. The spike and RdRp genes were simulated separately. Purifying selection was simulated across both genes. Evolution was simulated in the absence of recombination and with moderate and high levels of recombination during replication. Under each of these recombination paradigms, we simulated evolution in the absence of positive selection within

spike and with moderate and high levels of positive selection. Positive selection was simulated through exposure-dependent selection at a subset of spike S1 sites proportional to the number of epitope sites in H3N2 HA (Luksza and Lässig 2014). The simulated selection allows mutations in these “epitope” sites to rise in frequency while also encouraging “epitopes” to change over time (to mimic antigenic novelty). All simulations were run with a nucleotide mutation rate of 1x10-4 (Vijgen et al. 2005). Config files, results and source code for these simulations can be at `santa-sim_oc43a/` and the Bhatt method is implemented on the simulated data in `antigenic_evolution/bhatt_simulated_oc43_data.ipynb`.

Estimation of TMRCA

Mean TMRCA values were estimated for each gene and each HCoV using PACT (Bedford, Cobey, and Pascual 2011). Briefly, PACT computes TMRCA values by creating a series of subtrees that include only tips positioned within a temporal slice of the full tree and finding the common ancestor of these tips. The overall mean and 95% confidence interval were calculated from the list of TMRCA values in these time slices. The PACT config files and results for each run are in the directory `antigenic_evolution/pact/`. The TMRCA estimations and subsequent analyses are executed by code in `antigenic_evolution/tmrca_pact.ipynb`.

Acknowledgments

We thank Jesse Bloom and members of the Bedford lab for useful feedback. KEK was supported by the National Science Foundation Graduate Research Fellowship Program under Grant No. DGE-1762114. TB is a Pew Biomedical Scholar and is supported by NIH R35 GM119774-01.

Competing Interests

The authors declare no competing interests.

Figure Supplements

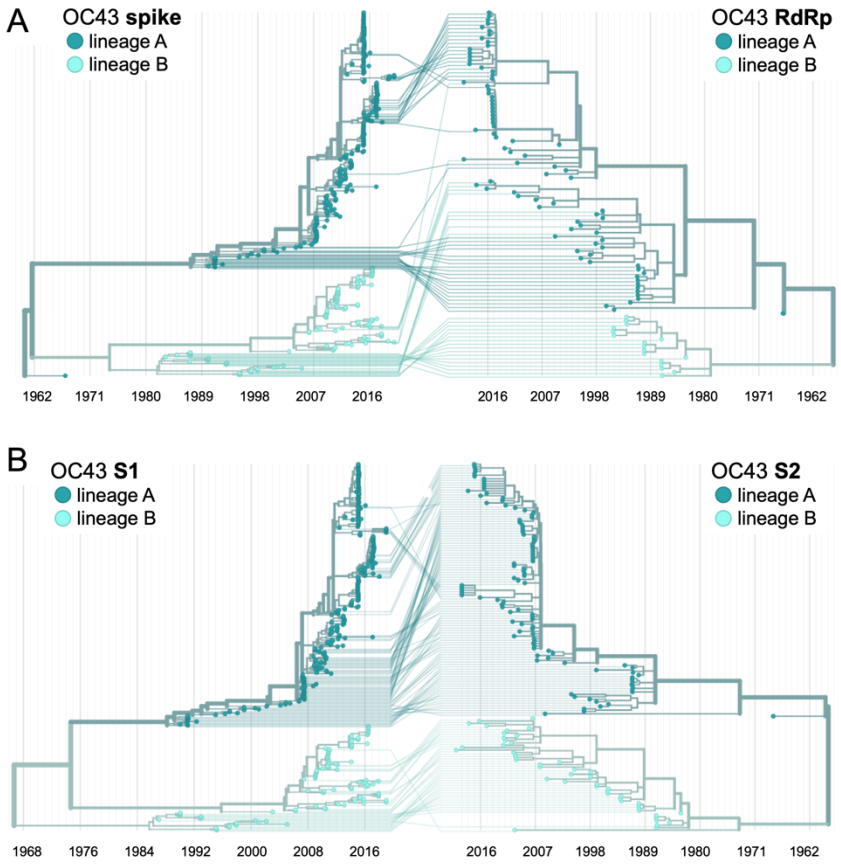

Figure 1- figure supplement 1. Recombination occurs between HCoV isolates. A tanglegram draws lines between an isolate's position on two phylogenies built on different genes (or genomic regions). Dramatic differences in an isolate's position on one tree versus another is indicative of recombination. A) Phylogenetic relationships between OC43 isolates based on spike sequences (left) versus relationships based on RdRp sequences (right). Light teal lines that connect isolates classified as lineage A based on their RdRp sequence to isolates classified as lineage B based on their spike sequence suggest that recombination occurred in these isolates or their ancestors. B) Phylogenetic reconstruction of OC43 isolates based on S1 sequences (left) versus S2 sequences (right). Year is shown on the x-axis.

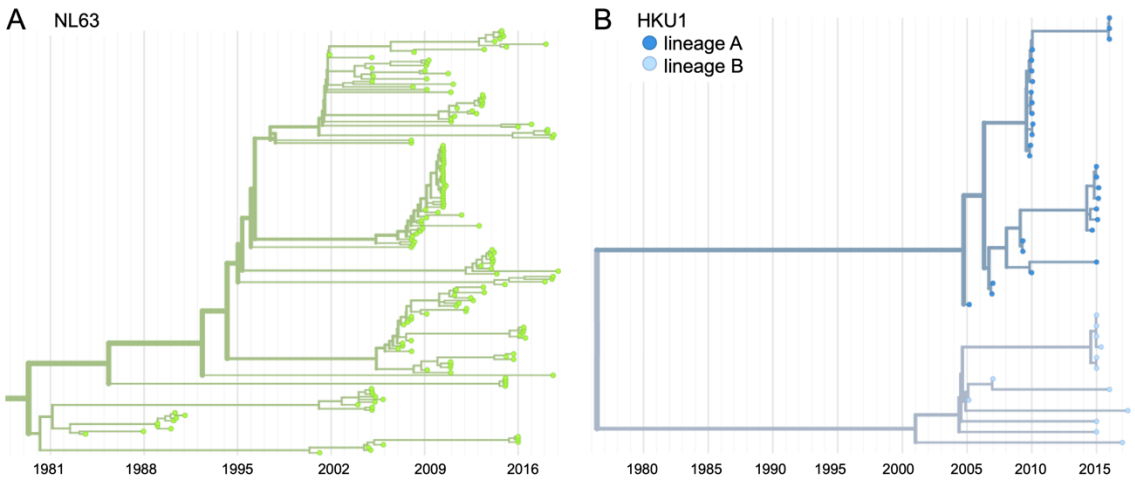

Figure 1- figure supplement 2. Phylogenetic trees for seasonal HCoVs NL63 and HKU1. Phylogenies built from A: NL63 spike sequences from 159 isolates over 37 years, and B: HKU1 spike sequences from 41 isolates over 13 years. HKU1 bifurcate immediately after the root and is split into lineage A (darker blue) and lineage B (lighter blue). NL63 contains just one lineage (green). Both HCoVs are rooted on an outgroup sequence. For the analyses in this paper, the evolution of each gene (or genomic region) is considered separately, so phylogenies are built for each viral gene and those phylogenies are used to split isolates into lineages for each gene. These are temporally resolved phylogenies with year shown on the x-axis. The clock rate of each HCoV is listed in the Methods “Phylogenetic inference” section.

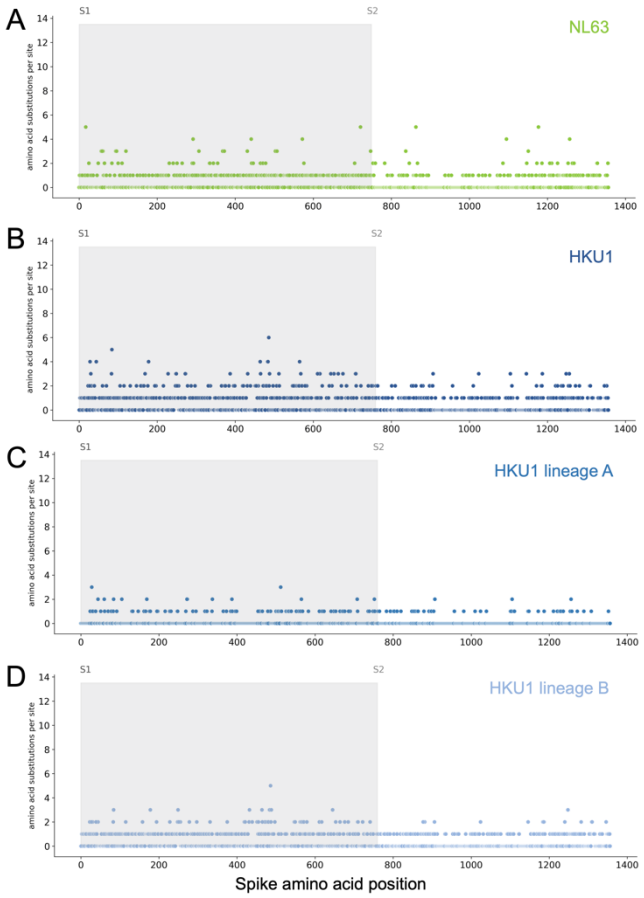

Figure 2- figure supplement 1. Mutations per at each position within Spike for NL63 and HKU1. Number of substitutions observed at each amino acid position in the spike gene throughout the phylogeny S1 (gray) and S2 (white) are indicated by shading and the number of substitutions per site is indicated by a dot and color-coded by HCoV lineage.. A: NL63, B: HKU1 (assuming all HKU1 isolates are a single lineage), C: HKU1 lineage A, D: HKU1 lineage B (assuming there are 2 co-circulating HKU1 lineages).

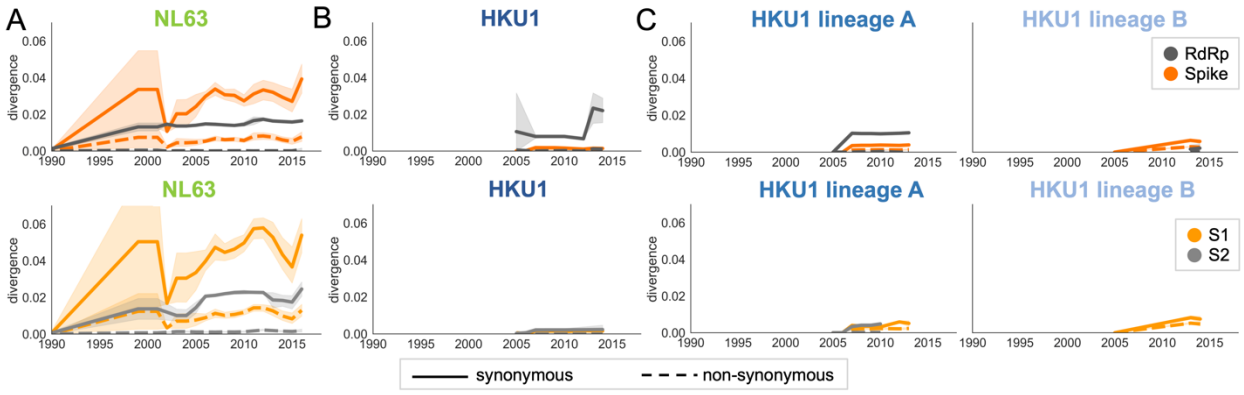

Figure 3- figure supplement 1. Nonsynonymous divergence in NL63 and HKU1. Nonsynonymous (dashed lines) and synonymous divergence (solid lines) within the spike (dark orange) and RdRp (dark gray) genes and within S1 (light orange) and S2 (light gray) over time. Divergence is the average Hamming distance from the ancestral sequence, computed in sliding 3-year windows which contain at least 2 sequenced isolates. Shaded region shows 95% confidence intervals. A: NL63, B: HKU1 (assuming all HKU1 isolates belong to a single lineage), and C: HKU1 (divided into 2 co-circulating lineages). Year is shown on the x-axis. Note that x- and y-axis scales are shared between the subplots but are different than Figure 3.

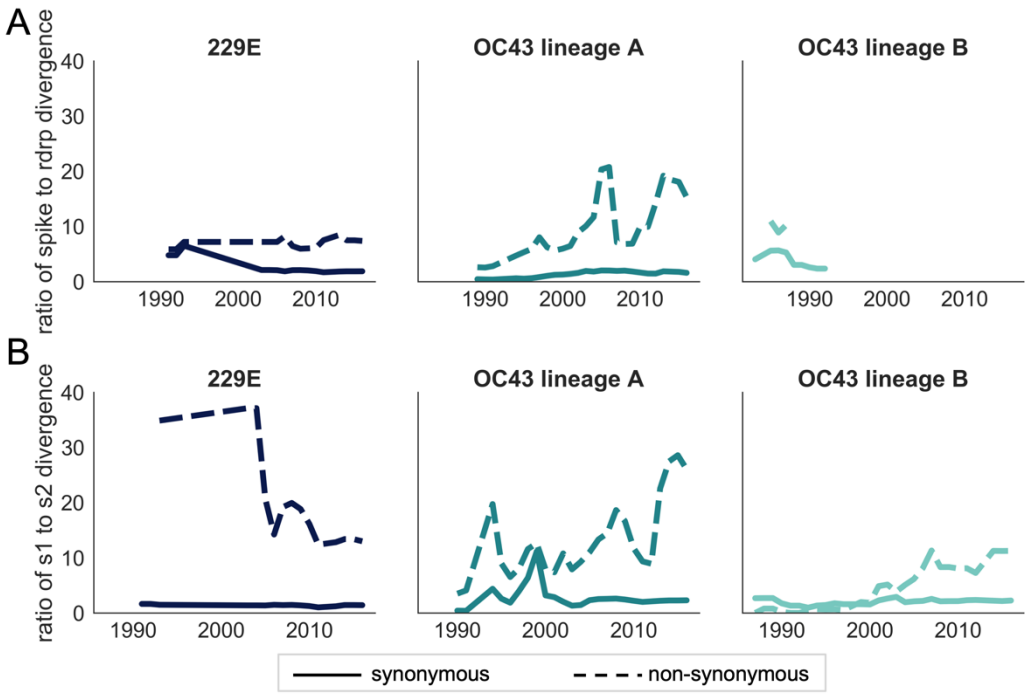

Figure 3- figure supplement 2. Ratio of divergence between genomic regions. A: the ratio of nonsynonymous divergence in spike to nonsynonymous divergence in RdRp (dashed lines) and the equivalent ratio of synonymous divergence (solid lines) is shown for 229E (dark blue), OC43 lineage A (dark teal), and OC43 lineage B (light teal). B: the same ratios of divergence as in panel A, except comparing S1 and S2. Year is on the x-axis.

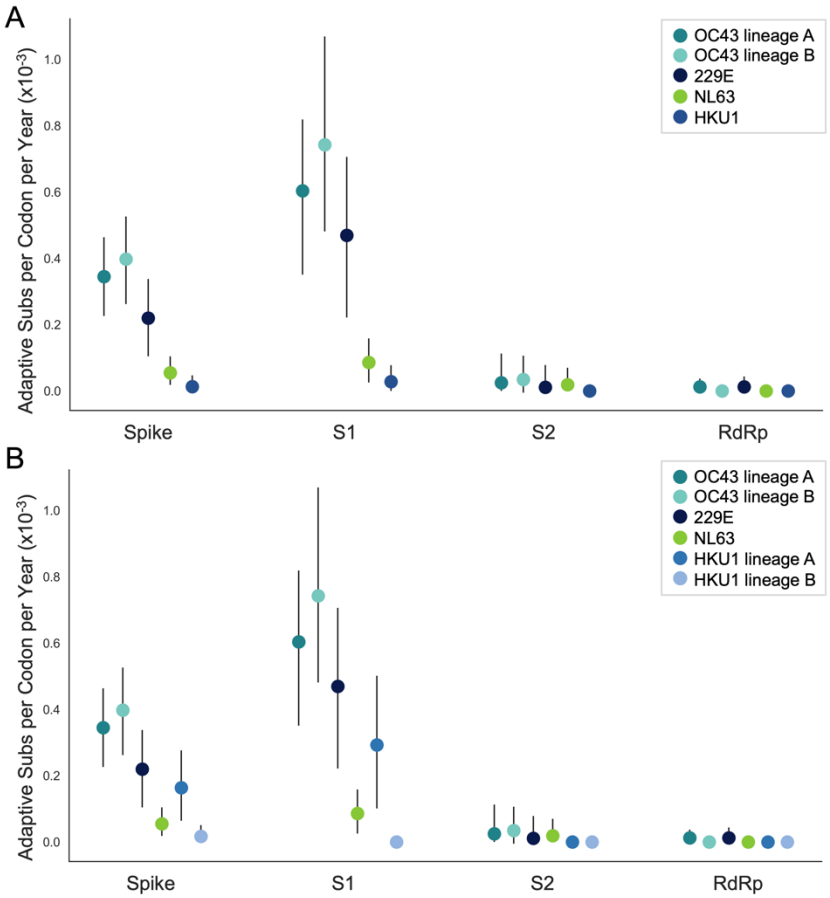

Figure 5- figure supplement 1. NL63 and HKU1 have low rates of adaptation in spike. As in Figure 4, adaptive substitutions per codon per year are calculated by our implementation of the Bhatt method. A: NL63 (green) and HKU1 (blue) are both considered to consist of a single lineage. B: HKU1 is divided into 2 co-circulating lineages (blue and light blue). The calculated rates of adaptive substitution within spike, S1, S2 and RdRp are plotted alongside 229E and OC43 for comparison. Error bars show 95% bootstrap percentiles from 100 bootstrapped datasets

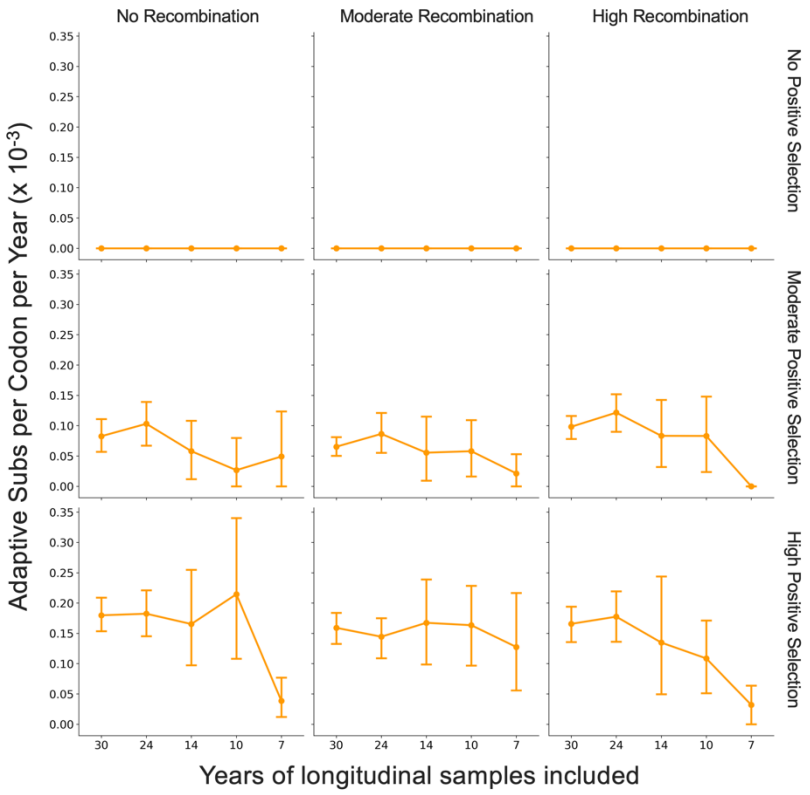

Figure 7- figure supplement 1. Fewer years of longitudinally-sampled isolates reduces ability to detect rate of adaptation. OC43 lineage A S1 sequences were simulated under conditions of no, moderate and high rates of recombination in combination with no, moderate or high strength of positive selection. The Bhatt method was used to calculate the ”true” rate of adaptive evolution under each of these scenarios using all available simulated sequence data (30 years), or the estimated rate if only the most recent 24, 14, 10 or 7 years of simulated sequences were used. The mean and 95% confidence intervals of 10 independent simulations are plotted.

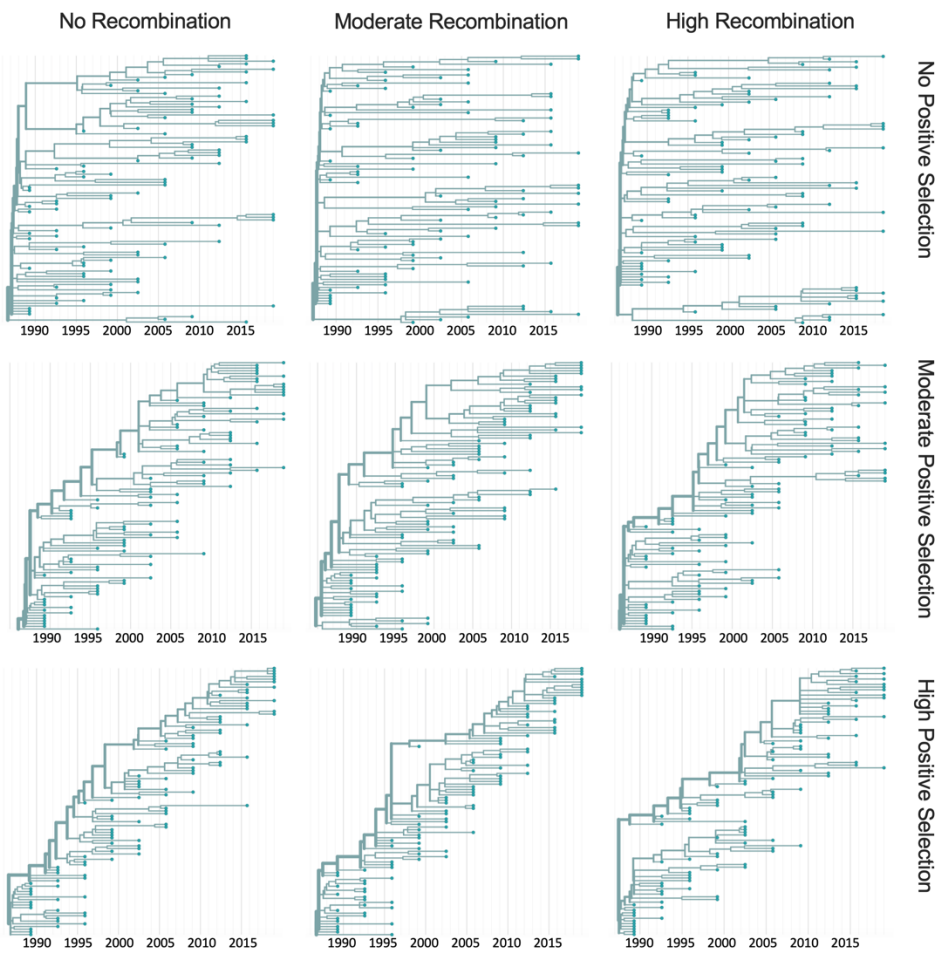

Figure 7- figure supplement 2. Representative phylogenies of simulated spike data. OC43 lineage A spike sequence evolution was simulated under conditions of no, moderate and high rates of recombination in combination with no, moderate or high strength of positive selection. This figure shows time-resolved phylogenies built from 1 of the 10 independent simulations under each recombination/selection regime.

References

Bedford, Trevor, Sarah Cobey, and Mercedes Pascual. 2011. “Strength and Tempo of Selection Revealed in Viral Gene Genealogies.”

Bedford, Trevor, Marc A. Suchard, Philippe Lemey, Gytis Dudas, Victoria Gregory, Alan J. Hay, John W. McCauley, Colin A. Russell, Derek J. Smith, and Andrew Rambaut. 2014. “Integrating Influenza Antigenic Dynamics with Molecular Evolution.” *ELife* 3 (February): e01914.

Bhatt, Samir, Edward C. Holmes, and Oliver G. Pybus. 2011. “The Genomic Rate of Molecular Adaptation of the Human Influenza A Virus.” *Molecular Biology and Evolution* 28 (9): 2443–51.

Bhatt, Samir, Aris Katzourakis, and Oliver G. Pybus. 2010. “Detecting Natural Selection in RNA Virus Populations Using Sequence Summary Statistics.” *Infection, Genetics and Evolution: Journal of Molecular Epidemiology and Evolutionary Genetics in Infectious Diseases* 10 (3): 421–30.

Bouckaert, Remco, Timothy G. Vaughan, Joëlle Barido-Sottani, Sebastián Duchêne, Mathieu Fourment, Alexandra Gavryushkina, Joseph Heled, et al. 2019. “BEAST 2.5: An Advanced Software Platform for Bayesian Evolutionary Analysis.” *PLoS Computational Biology* 15 (4): e1006650.

Chibo, Doris, and Chris Birch. 2006. “Analysis of Human Coronavirus 229E Spike and Nucleoprotein Genes Demonstrates Genetic Drift between Chronologically Distinct Strains.” *The Journal of General Virology* 87 (Pt 5): 1203–8.

Dorp, Lucy van, Damien Richard, Cedric C. S. Tan, Liam P. Shaw, Mislav Acman, and François Balloux. 2020. “No Evidence for Increased Transmissibility from Recurrent Mutations in SARS-CoV-2.” *Nature Communications* 11 (1): 5986.

Drake, J. W. 1993. “Rates of Spontaneous Mutation among RNA Viruses.” *Proceedings of the National Academy of Sciences of the United States of America* 90 (9): 4171–75.

Edridge, Arthur W. D., Joanna Kaczorowska, Alexis C. R. Hoste, Margreet Bakker, Michelle Klein, Katherine Loens, Maarten F. Jebbink, et al. 2020. “Seasonal Coronavirus Protective Immunity Is Short-Lasting.” *Nature Medicine*, September. https://doi.org/10.1038/s41591-020-1083-1.

Fulton, Benjamin O., David Sachs, Shannon M. Beaty, Sohui T. Won, Benhur Lee, Peter Palese, and Nicholas S. Heaton. 2015a. “Mutational Analysis of Measles Virus Suggests Constraints on Antigenic Variation of the Glycoproteins.” *Cell Reports* 11 (9): 1331–38.

———. 2015b. “Mutational Analysis of Measles Virus Suggests Constraints on Antigenic Variation of the Glycoproteins.” *Cell Reports* 11 (9): 1331–38.

Hadfield, James, Colin Megill, Sidney M. Bell, John Huddleston, Barney Potter, Charlton Callender, Pavel Sagulenko, Trevor Bedford, and Richard A. Neher. 2018. “Nextstrain: Real-Time Tracking of Pathogen Evolution.” *Bioinformatics* 34 (23): 4121–23.

Hamre, D., and M. Beem. 1972. “Virologic Studies of Acute Respiratory Disease in Young Adults. V. Coronavirus 229E Infections during Six Years of Surveillance.” *American Journal of Epidemiology* 96 (2): 94–106.

Heikkinen, Terho, and Asko Järvinen. 2003. “The Common Cold.” *The Lancet* 361 (9351): 51–59.

Hofmann, Heike, Graham Simmons, Andrew J. Rennekamp, Chawaree Chaipan, Thomas Gramberg, Elke Heck, Martina Geier, et al. 2006. “Highly Conserved Regions within the Spike Proteins of Human Coronaviruses 229E and NL63 Determine Recognition of Their Respective Cellular Receptors.” *Journal of Virology* 80 (17): 8639–52.

Hon, Chung-Chau, Tsan-Yuk Lam, Zheng-Li Shi, Alexei J. Drummond, Chi-Wai Yip, Fanya

Zeng, Pui-Yi Lam, and Frederick Chi-Ching Leung. 2008. “Evidence of the Recombinant Origin of a Bat Severe Acute Respiratory Syndrome (SARS)-like Coronavirus and Its Implications on the Direct Ancestor of SARS Coronavirus.” *Journal of Virology* 82 (4): 1819–26.

Hulswit, Ruben J. G., Yifei Lang, Mark J. G. Bakkers, Wentao Li, Zeshi Li, Arie Schouten, Bram Ophorst, et al. 2019. “Human Coronaviruses OC43 and HKU1 Bind to 9-O-Acetylated Sialic Acids via a Conserved Receptor-Binding Site in Spike Protein Domain A.” *Proceedings of the National Academy of Sciences of the United States of America* 116 (7): 2681–90.

Jariani, Abbas, Christopher Warth, Koen Deforche, Pieter Libin, Alexei J. Drummond, Andrew Rambaut, Frederick A. Matsen Iv, and Kristof Theys. 2019. “SANTA-SIM: Simulating Viral Sequence Evolution Dynamics under Selection and Recombination.” *Virus Evolution* 5 (1): vez003.

Katoh, Kazutaka, Kazuharu Misawa, Kei-Ichi Kuma, and Takashi Miyata. 2002. “MAFFT: A Novel Method for Rapid Multiple Sequence Alignment Based on Fast Fourier Transform.” *Nucleic Acids Research* 30 (14): 3059–66.

Kiyuka, Patience K., Charles N. Agoti, Patrick K. Munywoki, Regina Njeru, Anne Bett, James R. Otieno, Grieven P. Otieno, et al. 2018. “Human Coronavirus NL63 Molecular Epidemiology and Evolutionary Patterns in Rural Coastal Kenya.” *The Journal of Infectious Diseases* 217 (11): 1728–39.

Komabayashi, Kenichi, Yohei Matoba, Shizuka Tanaka, Junji Seto, Yoko Aoki, Tatsuya Ikeda, Yoshitaka Shimotai, Yoko Matsuzaki, Tsutomu Itagaki, and Katsumi Mizuta. 2020. “Longitudinal Epidemiology of Human Coronavirus OC43 in Yamagata, Japan, 2010–2017: Two Groups Based on Spike Gene Appear One after Another.” *Journal of Medical Virology* 7 (August): 825.

Kosakovsky Pond, Sergei L., David Posada, Michael B. Gravenor, Christopher H. Woelk, and Simon D. W. Frost. 2006. “Automated Phylogenetic Detection of Recombination Using a Genetic Algorithm.” *Molecular Biology and Evolution* 23 (10): 1891–1901.

Köster, Johannes, and Sven Rahmann. 2012. “Snakemake—a Scalable Bioinformatics Workflow Engine.” *Bioinformatics* 28 (19): 2520–22.

Krammer, Florian. 2020. “SARS-CoV-2 Vaccines in Development.” *Nature*, September. https://doi.org/10.1038/s41586-020-2798-3.

Kucharski, Adam J., Justin Lessler, Jonathan M. Read, Huachen Zhu, Chao Qiang Jiang, Yi Guan, Derek A. T. Cummings, and Steven Riley. 2015. “Estimating the Life Course of Influenza A(H3N2) Antibody Responses from Cross-Sectional Data.” *PLOS Biology*. https://doi.org/10.1371/journal.pbio.1002082.

Lau, Susanna K. P., Paul Lee, Alan K. L. Tsang, Cyril C. Y. Yip, Herman Tse, Rodney A. Lee, Lok-Yee So, et al. 2011. “Molecular Epidemiology of Human Coronavirus OC43 Reveals Evolution of Different Genotypes over Time and Recent Emergence of a Novel Genotype Due to Natural Recombination.” *Journal of Virology* 85 (21): 11325–37.

Li, Fang. 2016. “Structure, Function, and Evolution of Coronavirus Spike Proteins.” *Annual Review of Virology* 3 (1): 237–61.

Li, Zhijie, Aidan Ca Tomlinson, Alan Hm Wong, Dongxia Zhou, Marc Desforges, Pierre J. Talbot, Samir Benlekbir, John L. Rubinstein, and James M. Rini. 2019. “The Human Coronavirus HCoV-229E S-Protein Structure and Receptor Binding.” *ELife* 8 (October). https://doi.org/10.7554/eLife.51230.

Liu, Ding X., Jia Q. Liang, and To S. Fung. 2020. “Human Coronavirus-229E, -OC43, -NL63, and -HKU1.” *Reference Module in Life Sciences*. https://doi.org/10.1016/b978-0-12-809633-8.21501-x.

Liu, Lihong, Pengfei Wang, Manoj S. Nair, Jian Yu, Micah Rapp, Qian Wang, Yang Luo, et al. 2020. “Potent Neutralizing Antibodies against Multiple Epitopes on SARS-CoV-2 Spike.”

Nature 584 (7821): 450–56.
Luksza, Marta, and Michael Lässig. 2014. “A Predictive Fitness Model for Influenza.” *Nature* 507 (7490): 57–61.
McIntosh, Kenneth. 1974. “Coronaviruses: A Comparative Review.” In *Current Topics in Microbiology and Immunology / Ergebnisse Der Mikrobiologie Und Immunitätsforschung*, 85–129. Springer Berlin Heidelberg.
Monto, Arnold S., and Sook K. Lim. 1974. “The Tecumseh Study of Respiratory Illness. VI. Frequency of and Relationship between Outbreaks of Coronavims Infection.” *The Journal of Infectious Diseases* 129 (3): 271–76.
Murrell, Ben, Joel O. Wertheim, Sasha Moola, Thomas Weighill, Konrad Scheffler, and Sergei L. Kosakovsky Pond. 2012. “Detecting Individual Sites Subject to Episodic Diversifying Selection.” *PLoS Genetics* 8 (7): e1002764.
Nguyen, Lam-Tung, Heiko A. Schmidt, Arndt von Haeseler, and Bui Quang Minh. 2015. “IQ-TREE: A Fast and Effective Stochastic Algorithm for Estimating Maximum-Likelihood Phylogenies.” *Molecular Biology and Evolution* 32 (1): 268–74.
Pasternak, Alexander O., Willy J. M. Spaan, and Eric J. Snijder. 2006. “Nidovirus Transcription: How to Make Sense…?” *The Journal of General Virology* 87 (6): 1403–21.
Pickett, Brett E., Eva L. Sadat, Yun Zhang, Jyothi M. Noronha, R. Burke Squires, Victoria Hunt, Mengya Liu, et al. 2012. “ViPR: An Open Bioinformatics Database and Analysis Resource for Virology Research.” *Nucleic Acids Research* 40 (Database issue): D593-8.
Rambaut, Andrew, Oliver G. Pybus, Martha I. Nelson, Cecile Viboud, Jeffery K. Taubenberger, and Edward C. Holmes. 2008. “The Genomic and Epidemiological Dynamics of Human Influenza A Virus.” *Nature* 453 (7195): 615–19.
Reed, Sylvia E. 1984. “The Behaviour of Recent Isolates of Human Respiratory Coronavirus in Vitro and in Volunteers: Evidence of Heterogeneity among 229E-Related Strains.” *Journal of Medical Virology* 13 (2): 179–92.
Ren, Lili, Yue Zhang, Jianguo Li, Yan Xiao, Jing Zhang, Ying Wang, Lan Chen, Gláucia Paranhos-Baccalà, and Jianwei Wang. 2015. “Genetic Drift of Human Coronavirus OC43 Spike Gene during Adaptive Evolution.” *Scientific Reports* 5 (June): 11451.
Sagulenko, Pavel, Vadim Puller, and Richard A. Neher. 2018. “TreeTime: Maximum-Likelihood Phylodynamic Analysis.” *Virus Evolution* 4 (1): vex042.
Smith, Derek J., Alan S. Lapedes, Jan C. de Jong, Theo M. Bestebroer, Guus F. Rimmelzwaan, Albert D. M. E. Osterhaus, and Ron A. M. Fouchier. 2004. “Mapping the Antigenic and Genetic Evolution of Influenza Virus.” *Science* 305 (5682): 371–76.
Vijgen, Leen, Philippe Lemey, Els Keyaerts, and Marc Van Ranst. 2005. “Genetic Variability of Human Respiratory Coronavirus OC43.” *Journal of Virology*.
Volz, Erik M., Katia Koelle, and Trevor Bedford. 2013. “Viral Phylodynamics.” *PLoS Computational Biology* 9 (3): e1002947.
Weaver, Steven, Stephen D. Shank, Stephanie J. Spielman, Michael Li, Spencer V. Muse, and Sergei L. Kosakovsky Pond. 2018. “Datamonkey 2.0: A Modern Web Application for Characterizing Selective and Other Evolutionary Processes.” *Molecular Biology and Evolution*. https://doi.org/10.1093/molbev/msx335.
Woo, Patrick C. Y., Susanna K. P. Lau, Yi Huang, and Kwok-Yung Yuen. 2009. “Coronavirus Diversity, Phylogeny and Interspecies Jumping.” *Experimental Biology and Medicine* 234 (10): 1117–27.
Yang, Z. 2000. “Maximum Likelihood Estimation on Large Phylogenies and Analysis of Adaptive Evolution in Human Influenza Virus A.” *Journal of Molecular Evolution* 51 (5): 423–32.
Zanini, Fabio, Johanna Brodin, Lina Thebo, Christa Lanz, Göran Bratt, Jan Albert, and Richard A. Neher. 2015. “Population Genomics of Intrapatient HIV-1 Evolution.” *ELife* 4 (December). https://doi.org/10.7554/eLife.11282.
Zhang, Senyan, Panpan Zhou, Pengfei Wang, Yangyang Li, Liwei Jiang, Wenxu Jia, Han

Wang, et al. 2018. “Structural Definition of a Unique Neutralization Epitope on the Receptor-Binding Domain of MERS-CoV Spike Glycoprotein.” *Cell Reports*. https://doi.org/10.1016/j.celrep.2018.06.041.

Zhang, Yue, Jianguo Li, Yan Xiao, Jing Zhang, Ying Wang, Lan Chen, Gláucia Paranhos-Baccalà, Lili Ren, and Jianwei Wang. 2015. “Genotype Shift in Human Coronavirus OC43 and Emergence of a Novel Genotype by Natural Recombination.” *Journal of Infection*. https://doi.org/10.1016/j.jinf.2014.12.005.

Zhou, Haixia, Yingzhu Chen, Shuyuan Zhang, Peihua Niu, Kun Qin, Wenxu Jia, Baoying Huang, et al. 2019. “Structural Definition of a Neutralization Epitope on the N-Terminal Domain of MERS-CoV Spike Glycoprotein.” *Nature Communications*. https://doi.org/10.1038/s41467-019-10897-4.

Zhu, Yun, Changchong Li, Li Chen, Baoping Xu, Yunlian Zhou, Ling Cao, Yunxiao Shang, et al. 2018. “A Novel Human Coronavirus OC43 Genotype Detected in Mainland China.” *Emerging Microbes & Infections* 7 (1): 173.